



HAL
open science

Intestinal NAPE-PLD contributes to short-term regulation of food intake via gut-to-brain axis

Marialetizia Rastelli, Matthias van Hul, Romano Terrasi, Charlotte Lefort, Marion Regnier, Daniel Beiroa, Nathalie M. Delzenne, Amandine Everard, Ruben Nogueiras, Serge Luquet, et al.

► **To cite this version:**

Marialetizia Rastelli, Matthias van Hul, Romano Terrasi, Charlotte Lefort, Marion Regnier, et al.. Intestinal NAPE-PLD contributes to short-term regulation of food intake via gut-to-brain axis. *AJP - Endocrinology and Metabolism*, 2020, 319 (3), pp.E647-E657. 10.1152/ajpendo.00146.2020 . hal-03300410

HAL Id: hal-03300410

<https://cnrs.hal.science/hal-03300410>


Submitted on 15 Nov 2022

HAL is a multi-disciplinary open access archive for the deposit and dissemination of scientific research documents, whether they are published or not. The documents may come from teaching and research institutions in France or abroad, or from public or private research centers.

L'archive ouverte pluridisciplinaire **HAL**, est destinée au dépôt et à la diffusion de documents scientifiques de niveau recherche, publiés ou non, émanant des établissements d'enseignement et de recherche français ou étrangers, des laboratoires publics ou privés.

RESEARCH ARTICLE

Intestinal NAPE-PLD contributes to short-term regulation of food intake via gut-to-brain axis

Marialetizia Rastelli,¹ Matthias Van Hul,¹ Romano Terrasi,²  Charlotte Lefort,¹ Marion Régnier,¹ Daniel Beiroa,^{4,5} Nathalie M. Delzenne,¹ Amandine Everard,¹ Rubén Nogueiras,^{4,5} Serge Luquet,³  Giulio G. Muccioli,² and  Patrice D. Cani¹

¹Metabolism and Nutrition Research Group, Louvain Drug Research Institute, Walloon Excellence in Life sciences and BIOTEchnology (WELBIO), UCLouvain, Université catholique de Louvain, Bruxelles, Belgium; ²Bioanalysis and Pharmacology of Bioactive Lipids Research Group, Louvain Drug Research Institute, UCLouvain, Université catholique de Louvain, Bruxelles, Belgium; ³Université de Paris, BFA, UMR 8251, CNRS, Paris, France; ⁴Department of Physiology, CIMUS, University of Santiago de Compostela-Instituto de Investigación Sanitaria, Santiago de Compostela, Spain; and ⁵CIBER Fisiopatología de la Obesidad y Nutrición (CIBERObn), Santiago de Compostela, Spain

Submitted 9 April 2020; accepted in final form 27 July 2020

Rastelli M, Van Hul M, Terrasi R, Lefort C, Régnier M, Beiroa D, Delzenne NM, Everard A, Nogueiras R, Luquet S, Muccioli GG, Cani PD. Intestinal NAPE-PLD contributes to short-term regulation of food intake via gut-to-brain axis. *Am J Physiol Endocrinol Metab* 319: E647–E657, 2020. First published August 10, 2020; doi:10.1152/ajpendo.00146.2020.—Our objective was to explore the physiological role of the intestinal endocannabinoids in the regulation of appetite upon short-term exposure to high-fat-diet (HFD) and understand the mechanisms responsible for aberrant gut-brain signaling leading to hyperphagia in mice lacking *Napepld* in the intestinal epithelial cells (IECs). We generated a murine model harboring an inducible NAPE-PLD deletion in IECs (*Napepld*^{ΔIEC}). After an overnight fast, we exposed wild-type (WT) and *Napepld*^{ΔIEC} mice to different forms of lipid challenge (HFD or gavage), and we compared the modification occurring in the hypothalamus, in the vagus nerve, and at endocrine level 30 and 60 min after the stimulation. *Napepld*^{ΔIEC} mice displayed lower hypothalamic levels of *N*-oleoylethanolamine (OEA) in response to HFD. Lower mRNA expression of anorexigenic *Pomc* occurred in the hypothalamus of *Napepld*^{ΔIEC} mice after lipid challenge. This early hypothalamic alteration was not the consequence of impaired vagal signaling in *Napepld*^{ΔIEC} mice. Following lipid administration, WT and *Napepld*^{ΔIEC} mice had similar portal levels of glucagon-like peptide-1 (GLP-1) and similar rates of GLP-1 inactivation. Administration of exendin-4, a full agonist of GLP-1 receptor (GLP-1R), prevented the hyperphagia of *Napepld*^{ΔIEC} mice upon HFD. We conclude that in response to lipid, *Napepld*^{ΔIEC} mice displayed reduced OEA in brain and intestine, suggesting an impairment of the gut-brain axis in this model. We speculated that decreased levels of OEA likely contributes to reduce GLP-1R activation, explaining the observed hyperphagia in this model. Altogether, we elucidated novel physiological mechanisms regarding the gut-brain axis by which intestinal NAPE-PLD regulates appetite rapidly after lipid exposure.

appetite regulation; gut-to-brain axis; dietary lipid; NAPE-PLD; *N*-acylethanolamines

INTRODUCTION

Feeding and energy homeostasis are essential life processes that every living organism must attain to survive. Among the different regulatory pathways involved, the endocannabinoid

system (ECS) functions as a potent regulator of feeding behavior and energy balance. The ECS is composed of bioactive lipid mediators, their membrane-associated and nuclear receptors, and enzymes involved in the synthesis and degradation of these mediators (45).

N-acylethanolamines (NAEs) are a subgroup of bioactive lipids belonging to the ECS that share structural similarities having a common ethanolamide moiety linked to a specific fatty acid. The levels of NAEs are tightly regulated by on-demand synthesis from membrane phospholipids and rapid degradation (30). *N*-acylphosphatidylethanolamine phospholipase D (NAPE-PLD) is considered the main synthesizing enzyme for NAEs, although studies using total *Napepld* knockout (*NAPE-PLD*^{-/-}) mice have suggested the existence of alternative pathways (29). Hydrolysis of NAEs is mediated by fatty acid amide hydrolase (FAAH) and *N*-acylethanolamine acid amidase (NAAA) (33, 50).

The most studied NAE is *N*-arachidonylethanolamine (AEA; also called anandamide), and it has been implicated in the regulation of appetite and energy homeostasis (6). Other members of the NAE cluster, such as *N*-oleoylethanolamine (OEA), *N*-palmitoylethanolamine (PEA), and *N*-stearoylethanolamine (SEA), are also involved in modulation of appetite, lipid metabolism, and inflammation (13, 21, 41).

It has been suggested that intestinal NAEs play a role in the control of both food intake and whole body energy homeostasis (9, 20, 22). Among them, OEA contributes to the modulation of appetite and glucose homeostasis. The anorectic effect of OEA has been widely established in rodents (16, 17, 20, 39, 41, 47). This is mediated through direct activation of peroxisome proliferator-activated receptor- α (PPAR α) (15). Additionally, OEA indirectly modulates appetite and glucose homeostasis by activating the GPR119 receptor expressed on enteroendocrine (EECs) L cells, thereby stimulating the secretion of glucagon-like peptide-1 (GLP-1) (27), which in turn controls glucose homeostasis and appetite (34).

However, the exact molecular mechanisms regulating the production of these intestinal NAEs are still being debated. In addition, data indicate that dysregulation of the intestinal ECS might play a role in obesity (25), thus confirming the importance of the intestinal ECS.

Correspondence: P. D. Cani (patrice.cani@uclouvain.be).

Given that whole body NAPE-PLD^{-/-} mice did not develop a clear phenotype and did not display reduced levels of NAEs in periphery (24, 29), we used tissue-specific approaches to capture in time and space the role of NAPE-PLD on metabolism. We previously demonstrated that deletion of NAPE-PLD specifically in the adipocytes induced obesity, glucose intolerance, and altered lipid metabolism under a normal diet (18). Recently, we generated a mouse model with an inducible deletion of NAPE-PLD in the intestinal epithelial cells (*Napepld*^{ΔIEC}) (14). We observed that upon long-term high-fat diet (HFD) feeding, *Napepld*^{ΔIEC} mice developed a stronger obese phenotype in comparison with the control mice together with stronger hepatic steatosis (14), suggesting that intestinal NAPE-PLD plays a role in the regulation of whole body energy homeostasis and lipid absorption.

We also discovered that intestinal epithelial NAPE-PLD plays a key role in short-term regulation of food intake upon exposure to lipid-rich diet (14). Indeed, *Napepld*^{ΔIEC} mice exposed to HFD consumed significantly more food than the WT mice within 4 h. The hyperphagia of *Napepld*^{ΔIEC} mice was associated with a lack of HFD-induced upregulation of anorectic proopiomelanocortin (POMC) mRNA in the hypothalamus. However, the mechanisms responsible for this alteration in the gut-to-brain axis are unknown. In addition, it is not clear whether impaired hypothalamic *Pomc* expression is a consequence of the hyperphagic response or the consequence of impaired intestinal response to lipids.

Therefore, we explored the dynamic response of intestinal cells and hypothalamic and vagal neurons to acute dietary fat exposure in WT and *Napepld*^{ΔIEC} mice.

MATERIALS AND METHODS

Mice

All mouse experiments were reviewed and approved by and performed in accordance with the guidelines of the local ethics committee for animal care of the Health Sector of the Université Catholique de Louvain under the supervision of P. D. Cani and J. P. Dehoux under the specific agreement number 2014/UCL/MD/022 and 2017/UCL/MD/005. Housing conditions were as specified by the Belgian Law of May 29, 2013, regarding the protection of laboratory animals (agreement no. LA1230314). Every effort was made to minimize animal pain, suffering, and distress. The studies were carried out following the ARRIVE guidelines.

Mouse data are expressed as means ± SE. The number of mice allocated per group was based on previous experiments investigating the effects of *Napepld* deletion in the intestinal epithelial cells (14). At the beginning of each experiment, animals were randomly assigned to experimental groups to ensure that each group was matched in terms of body weight and fat mass. No blinding procedure was followed. Any exclusion of mice and sample was based, on the one hand, on careful examination of mice and organ appearance during necropsy and sampling (for example, granulous liver) and, on the other hand, an outlier exclusion criteria supported by the use of the Grubbs' test.

All mice used in this study were littermates and bred in a specific and opportunistic pathogen-free (SOPF) animal facility.

Before the beginning of the experiments described below, the animals were housed in pairs in SOPF conditions and in a controlled environment (room temperature of 23 ± 2°C, 12-h daylight cycle) with free access to sterile food (irradiated) and sterile water. During acclimation, injections and washout period mice were fed a normal diet (ND; AIN93Mi; Research Diets, New Brunswick, NJ).

Generation of *Napepld*^{ΔIEC} Mice and Experimental Designs

All the animals used in this study have an inducible intestinal epithelial *Napepld*-deletion (*Napepld*^{ΔIEC}) on C57BL/6 background. These animals were generated in our laboratory, as previously described (14), by crossing mice bearing a tamoxifen-dependent Cre recombinase expressed under the control of the villin promoter (Villin Cre-ERT2) (kind gift of Dr. Sylvie Robine), with mice harboring a loxP-flanked *Napepld* allele (12).

At 7 wk of age, the animals were injected intraperitoneally (ip) for 5 consecutive days with 100 μL of vehicle (10% vol/vol EtOH in filtered sunflower oil) or with tamoxifen (10 mg/mL in vehicle) to obtain control mice (WT) or mice deleted for *Napepld* in the intestinal epithelial cells (*Napepld*^{ΔIEC}), respectively. Vehicle and tamoxifen solutions were prepared and stored as previously described (14).

At the end of each experiment, the successful deletion was routinely validated by quantitative PCR (qPCR) analysis in the small and large intestines of WT and *Napepld*^{ΔIEC} animals.

Experiment 1: short-term exposure to HFD. One cohort of 10-wk-old WT or *Napepld*^{ΔIEC} male mice (37 mice in total) was housed individually for 1 wk for acclimation. They were then split in four body weight-matched groups ($n = 8-10$ /group), fasted overnight (ON) during the dark phase and then either exposed for 4 h to HFD (60 kcal% fat and 20 kcal% carbohydrates, D12492; Research Diets) (WT HFD or *Napepld*^{ΔIEC} HFD) or maintained fasted for 4 h before anesthesia and tissue harvesting.

Experiment 2: acute oral lipid challenge. 11-wk-old WT or *Napepld*^{ΔIEC} male mice (43 mice in total) were split in six body weight-matched groups ($n = 6-8$ /group). After an ON fast during the dark phase, the animals received 300 μL of lipid-rich emulsion (FRESUBIN, 96.8% kcal% fat) by oral gavage, and tissues were harvested after exactly 30 min (WT 30' or *Napepld*^{ΔIEC} 30') or 1 h (WT 60' or *Napepld*^{ΔIEC} 60'). Control groups were force fed with 300 μL of NaCl (WT fasted or *Napepld*^{ΔIEC} fasted).

Experiment 3: neuronal activation in the NTS following HFD exposure. An additional cohort of WT and *Napepld*^{ΔIEC} male mice (21 mice; $n = 10$ and 11, respectively) was fasted ON during the dark phase and refed the following morning with HFD for 1 h. We chose to refeed the animals for 1 h, since evidence demonstrates that the expression of c-fos peaks at this time point (51). The animals were anesthetized with ip injection of ketamine-xylazine (100 mg/mL and 20 mg/mL, respectively), and tissue fixation was performed by cardiac perfusion with a solution of cold phosphate-buffered saline (PBS) followed by cold 4% (wt/vol) paraformaldehyde (PFA) solution. The brain was carefully harvested in its entirety, postfixed in 4% PFA ON at 4°C, cryoprotected ON at 4°C in a solution of sucrose 30% (wt/vol), and subsequently frozen in cold isopentane and stored at -80°C until cryosectioning.

Experiment 4: exendin-4 administration and individual measure of HFD intake. A fourth cohort of 11-wk-old WT or *Napepld*^{ΔIEC} male mice (28 mice) were individually housed for 1 wk for acclimation. The mice were then placed in metabolic chambers and allowed to adapt to the new environment for an additional 5 days with free access to ND and sterile water; during this period, the mice were accustomed to ip injection for 2 consecutive days by receiving a single sterile NaCl injection daily.

For the experiment, after an ON fast during the dark phase the animals were divided into four groups ($n = 7$ /group) and received vehicle (NaCl) or 0.06 μg of exendin-4 (Ex-4) (no. 4019602; Bachem) in 100 μL and immediately exposed to ad libitum HFD for 24 h. The submaximal dose of Ex-4 was chosen based on previous rodent studies (46). Using metabolic cages, food consumption was monitored at 15-min intervals. Consumption of food >0.5 g within the above-mentioned interval of time was considered as spillage, and the animal was excluded starting from that time point. No spillage was registered during the first 8 h of follow-up for any of the animals.

Tissue Sampling

Except for *experiment 3*, mice were anesthetized with isoflurane (Forene; Abbott, Queenborough, Kent, UK) at the end of the experience. Blood was sampled from the portal and cava veins. After exsanguination, mice were euthanized by cervical dislocation. Tissues were precisely dissected, immediately immersed in liquid nitrogen, and stored at -80°C for further analysis. For the investigation of the vagal response, the left and the right nodose ganglia were sampled from the neck of the mouse, snap frozen, and stocked at -80°C . For RNA purification, left and right nodose ganglia from one animal were pooled.

RNA Purification and RT-qPCR

Total RNA was prepared from tissues as previously described (14) using TriPure reagent (Roche). Quantification and integrity analysis of total RNA were performed by analyzing 1 μL of each sample in an Agilent 2100 Bioanalyzer (Agilent RNA 6000 Nano Kit; Agilent, Santa Clara, CA). cDNA was prepared by reverse transcription of 1 μg (or 0.2 μg for nodose ganglia) of total RNA using a Reverse Transcription System kit (Promega, Madison, WI). Real-time PCR was performed with the Quant Studio3 real-time PCR system and the QuantStudio software, as previously described (14). *Rpl19* RNA was chosen as housekeeping gene. The primer sequences for the targeted mouse genes are presented in Table 1.

NAEs Quantification

AEA and OEA measurements in jejunum and in plasma from cava vein were performed as previously described (14).

For NAE measurement in hypothalamus, following RNA extraction, the remaining solution was added to vials containing dichloromethane (CH_2Cl_2 ; 8 mL), methanol (MeOH; 4 mL; containing BHT), water (containing EDTA), and the internal standards (deuterated *N*-acylethanolamines, deuterated 2-AG). After the extraction, the organic phase was recovered and purified by solid phase extraction (36). The lipids of interest were recovered using hexane-isopropanol 7:3 (vol/vol) and analyzed by HPLC-MS/MS. The samples (1 μL) were injected on a Xevo TQ-S mass spectrometer equipped with an Acquity UPLC class H (both from Waters). An Acquity UPLC BEH C18 (2.1 \times 50 mm; 1.7 μm , kept at 40°C) column and a linear gradient (200 $\mu\text{L}/\text{min}$) between MeOH- H_2O -acetic acid (75:24.9:0.1; vol/vol/vol) and MeOH-acetic acid (99.9:0.1; vol/vol) were used for the separation. A quantification and a

qualification transition were optimized for the different NAEs and d-NAE, and the MassLynx software was used for data acquisition and processing. For each compound, the ratio between the area under the curve of the lipid and the area under the curve of the corresponding internal standard was used for data normalization. Calibration curves with a range going from 2.5 fmol to 800 fmol (values on column) were also obtained in the same conditions. The obtained values were then normalized to the tissue weight.

Protein Extraction and Western Blot Analysis

To obtain total protein lysates, tissues were homogenized with TissueLyser II (Qiagen) in RIPA buffer supplemented with a cocktail of protease inhibitors (Sigma) and phosphatase inhibitors. Equal amounts of proteins, as measured by the Pierce method (Pierce BCA Protein assay kit), were separated by SDS-PAGE (15% acrylamide) and transferred to PVDF membranes. Membranes were then incubated ON at 4°C with primary anti-POMC antibody (Ab94446; Abcam) diluted 1:1,000 in Tris-buffered saline Tween-20 containing 1% nonfat dry milk. The loading control was β -actin (1:10,000, ab6276; Abcam). The membranes were developed with the use of an ultrasensitive chemiluminescence protein dye detection system (ECL Plus; Amersham Pharmacia Biotech, Piscataway, NJ). The exposure time was between 5 and 7 s for revelation of POMC and 3–4 s for β -actin. The bands were subjected to semiquantitative analysis via ImageQuant software. The specificity of POMC primary antibody was previously validated by immunohistology (14) and confirmed here by the specific position of the band at the expected molecular weight.

Immunostaining: c-Fos Quantification in the Nucleus of the Solitary Tract

Twenty-micrometer-thick serial coronal cryosections were mounted on SuperFrost Plus slides (Menzel Gläser) and kept at -20°C until staining. For nucleus of the solitary tract (NTS), we harvested ~ 12 serial sections per animal from bregma -6.36 mm to -7.76 mm according to The Mouse Brain in stereotaxic coordinates (Paxinos and Franklin, 2004, Elsevier Science); c-fos immunohistochemistry was performed as previously described (14). Bright-field images of the NTS were obtained using a Leica SCN400 at $\times 10$ magnification. c-Fos-positive neurons were manually counted using Fiji software in a blinded manner. The region of interest (ROI) corresponding to the NTS was delimited on each section, using The Mouse Brain in Stereotaxic Coordinates (Paxinos and

Table 1. List of primers used

Gene	Forward 5'→3'	Reverse 5'→3'
<i>AgRP</i>	CGG AGG TGC TAG ATC CAC AGA	AGG ACT AGT GCA GCC TTA CAC
<i>Cart</i>	TTC CTG CAA TTC TTT CCT CTT GA	GGG AAT ATG GGA ACC GAA GGT
<i>Cckar</i>	ACA ATA ACC AGA CGG CGA AC	ATG AGT CCG TAA GCC ACC AC
<i>Cnr1</i>	CTG ATG TTC TGG ATC GGA GTC	TCT GAG GTG TGA ATG ATG ATG C
<i>Cpe</i>	AAG GGT TTG TCC GTG ACC TT	GTT TCA GGA GCA AGC AAT C
<i>Faah</i>	GTG AGG ATT TGT TCC GCT TG	GGA GTG GGC ATG GTG TAG TT
<i>Ghsh</i>	GGA AAC ATC AAA AGC CAA CC	TCC CAA GAA CTA GCG GAA GA
<i>Glp1r</i>	GGG CCA GTA GTG TGC TAC AA	CTT CAC ACT CCG ACA GGT CC
<i>Gpr119</i>	AGC TCT GCT CAG CAT ACA CAG	AAA TGC CAT CCG AAG GCT AC
<i>LepR</i>	ATC TGC CGG TGT GAG TTT TC	CTA AGG GTG GAT CGG GTT TC
<i>NaaA</i>	ATT ATG ACC ATT GGA AGC CTG CA	CGC TCA TCA CTG TAG TAT AAA TTG TGT AG
<i>Napepld</i>	TTC TTT GCT GGG GAT ACT GG	GCA AGG TCA AAA GGA CCA AA
<i>Nat1</i>	CCC CGA GTT ATC GAG GAT TT	CTG CAA GGA ACA GAA CGA TG
<i>Npy</i>	CAG AAA ACG CCC CCA GAA C	CGG GAG AAC AAG TTT CAT TTC C
<i>Pace4</i>	CGA AAC CCA GAG AAA CAA GG	ACT GAT GGG AGC TGA AGG TG
<i>Pam</i>	TAA AAA GGC TGG CAT TGA GG	TCT GAG GAG GTG GGT TTG TT
<i>Pcl</i>	GGC TGC TGG TAT CTT TGC TC	CCC CAT TCT TTT TCC AAC CT
<i>Pc2</i>	GGA GCT GGG ATA CAC AGG AA	CCA GGT CTG GGT GGA GAT AG
<i>Pomc</i>	AGG CCT GAC ACG TGG AAG AT	AGC AGG AGG GCC AGC AA
<i>Rpl19</i>	GAA GGT CAA AGG GAA TGT GTT CA	CCT TGT CTG CCT TCA GCT TGT
<i>Y2r</i>	AAC GCG CAA GAG TCA ATA CA	CCA TAG GGC TCC ACT TTC AC

The primers are listed in alphabetical order.

Franklin, 2004, Elsevier Science) as a reference. At least four brain sections were analyzed and averaged for each animal.

The specificity of the anti c-fos primary antibody (ab190289 from Abcam) was validated in a previous study (14).

Quantification of GLP-1 in Portal Plasma

For GLP-1 quantification, DPP-4 inhibitor (DPP4-010; Merck) was added to the portal blood during sampling at necropsy. GLP-1 was quantified in plasma using an ELISA kit (no. K1503PD; Meso Scale Delivery) according to the manufacturer's instructions.

Quantification of DPP-4 Activity

DPP-4 activity was measured in peripheral plasma by quantification of the cleavage of para-nitroanilide (PNA) from Gly-Pro-PNA (Sigma, St. Louis, MO). Samples (15 μ L) were diluted in TRIS-base buffer (50 mM, pH 8.3) and incubated with Gly-Pro-PNA. The enzymatic activity was measured in a kinetic analysis of 30 min at 37°C (380 nm) (SpectraMax M2; Molecular Devices, San Jose, CA) and quantified using a standard curve of free PNA.

Data Analysis and Statistics

Statistical analyses were performed using GraphPad Prism 8.1 (GraphPad Software, San Diego, CA). The statistical tools used for each analysis are specified in the figure captions. Differences with P values of <0.05 were considered significant.

RESULTS

The Endocannabinoid Tone is Altered in the Hypothalamus of *Napepld* ^{Δ IEC} Mice Following the Exposure to HFD

After confirming that *Napepld* ^{Δ IEC} mice ate significantly more in comparison with WT mice following 4 h of HFD exposure (Fig. 1A), we explored the mechanisms potentially involved in this behavior.

Although the deletion of the *Napepld* was restricted to the intestinal epithelial cells (Supplemental Fig. S1A; <https://doi.org/10.6084/m9.figshare.12666299>) (14), we investigated whether this could have a broader effect and lead to altered endocannabinoid tone in the hypothalamus of *Napepld* ^{Δ IEC} mice. Therefore, we measured the level of several NAEs in the hypothalamus of WT and *Napepld* ^{Δ IEC} mice following a fasting period and 4 h of HFD feeding.

In response to HFD exposure, WT mice displayed decreased AEA levels in the hypothalamus, whereas *Napepld* ^{Δ IEC} mice had increased AEA levels in hypothalamus after HFD feeding, thereby leading to 20% of difference between both groups (Fig. 1B). In addition, in response to HFD, hypothalamic OEA levels were decreased by $\sim 55\%$ in *Napepld* ^{Δ IEC} mice (Fig. 1C). These data strongly suggested an altered regulation of the orexigenic AEA and the anorexigenic OEA in response to HFD exposure in the hypothalamus of *Napepld* ^{Δ IEC} mice compared with WT mice.

The level of NAEs not primarily involved in regulation of food intake (namely PEA, SEA, NAE 20:0) were similar between WT and *Napepld* ^{Δ IEC} mice (Supplemental Fig. S1B). The endocannabinoid 2-arachidonoylglycerol (2-AG) also affects food intake; however, the levels of hypothalamic 2-AG were similar in WT and *Napepld* ^{Δ IEC} mice in response to HFD exposure (Supplemental Fig. S1B).

Moreover, the hypothalamic expression of NAE-synthetizing and -degrading enzymes was also differently regulated in WT and *Napepld* ^{Δ IEC} mice following HFD consumption (Fig. 1D). The expression of NAE-synthetizing *Nat1* was significantly up-regulated in *Napepld* ^{Δ IEC} mice in comparison with WT. *Napepld* followed the same trend without reaching significance ($P = 0.09$). In contrast, expression of *Faah*, a NAEs degrading protein, was significantly downregulated in *Napepld* ^{Δ IEC} mice in comparison with WT, whereas *Naaa* was not affected (Fig. 1D).

Interestingly, we also demonstrated that the effect on AEA and OEA levels in *Napepld* ^{Δ IEC} mice was specific to HFD exposure, since feeding with normal diet (ND) did not significantly affect NAE levels (Supplemental Fig. S1C). This suggests that the hypothalamic alteration of ECS occurs specifically upon lipid consumption.

Dysfunction of POMC Neurons Occurs Rapidly in the Hypothalamus of *Napepld* ^{Δ IEC} Mice in Response to Lipid Exposure

POMC neurons are key regulators of appetite in response to endocrine or nervous signals coming from the periphery (43). We previously observed that mice lacking *Napepld* in intestinal epithelial cells had altered activity of POMC neurons after 4 h

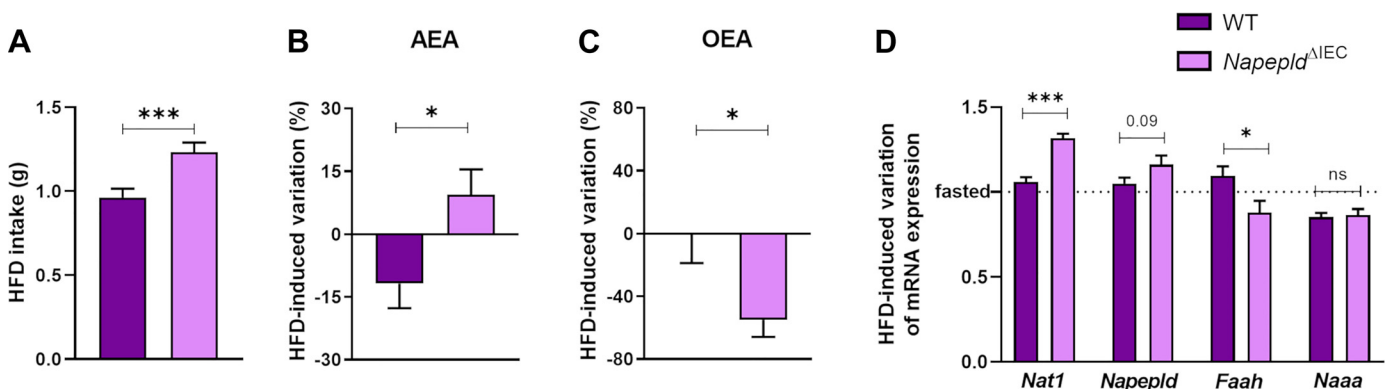


Fig. 1. The endocannabinoid tone is altered in the hypothalamus of *Napepld* ^{Δ IEC} mice following exposure to high-fat diet (HFD). A: *Napepld* ^{Δ IEC} mice are hyperphagic when exposed to lipid-rich diet ($n = 37-39$, pool of 4 separate experiments). B and C: hypothalamic levels of orexigenic *N*-arachidonylethanolamine (AEA; B) were increased and levels of anorexigenic *N*-oleoylethanolamine (OEA; C) were decreased in *Napepld* ^{Δ IEC} mice following consumption of HFD ($n = 7-8$). D: in response to HFD feeding, the transcription of enzymes belonging to the endocannabinoid system (ECS) was also differently modulated in WT and *Napepld* ^{Δ IEC} mice ($n = 7-9$). Data are expressed as means \pm SE. * $P < 0.05$ and *** $P < 0.001$ following unpaired Student's t -test.

of HFD exposure (14). Considering that hypothalamic neuropeptides rapidly change following nutritional challenge, we investigated the response of POMC neurons to dietary lipid at earlier time points. Therefore, we measured the transcription of *Pomc* already 30 and 60 min after oral lipid challenge.

In WT mice, lipid administration induced a progressive increase in *Pomc* transcription in the hypothalamus, with a 1.5-fold increase being reached after 60 min in comparison to WT fasted mice ($P = 0.01$, Mann-Whitney test). Conversely, in *Napepld*^{ΔIEC} mice, the hypothalamic transcription of *Pomc* remained unchanged over time and was significantly lower than in WT mice 60 min after the lipid load (Fig. 2A). Western blot analysis of POMC expression in the hypothalamus showed a similar trend (Supplemental Fig. S2A; <https://doi.org/10.6084/m9.figshare.12100824>).

The defect in lipid sensing was specific to the *Pomc* transcript, whereas the mRNA of none of the other appetite-regulating peptides in the arcuate (cocaine and amphetamine regulated transcript: *Cart*; neuropeptide Y: *Npy*; agouti-related protein: *Agrp*) was affected by the intestinal deletion of *Napepld* (Supplemental Fig. S2B). In addition, the transcriptional impairment specifically occurred in hypothalamic POMC neurons and not in POMC neurons of the hindbrain (Fig. 2B).

Posttranslational cleavage of POMC is finely regulated in response to energy requirements to optimally adapt the levels

of the different POMC-derived bioactive peptides such as appetite-suppressing α -melanocyte stimulating hormone (α -MSH) (40). We observed that the mRNA of the enzymes involved in posttranslational processing of POMC was not differently expressed in WT and *Napepld*^{ΔIEC} mice following lipid exposure (Fig. 2C).

Altogether, these data suggested that the intestinal deletion of *Napepld* impaired the response of anorectic POMC neurons to intestinal lipid already earlier than 4 h. We also demonstrated that the defect specifically involved POMC neurons in the hypothalamus, but not POMC neurons in the hindbrain.

Neither Vagal Plasticity Nor Vagal Signaling are Impaired by Intestinal Deletion of Napepld in Response to Lipid

Because the alteration of hypothalamic anorectic response in *Napepld*^{ΔIEC} mice occurred very rapidly, we hypothesized that an impaired transmission of nervous signals from the intestine to the brain could contribute to the observed phenotype.

Intestinal terminations of the vagus nerve express membrane receptors that mediate appetite-suppressing or appetite-stimulating signals in response to intestinal hormones, bioactive lipids, and macronutrients (11). The profile of receptors expressed is known to rapidly change in response to feeding (10).

We wondered whether the expression of those receptors was differently modulated in the nodose ganglia of WT and

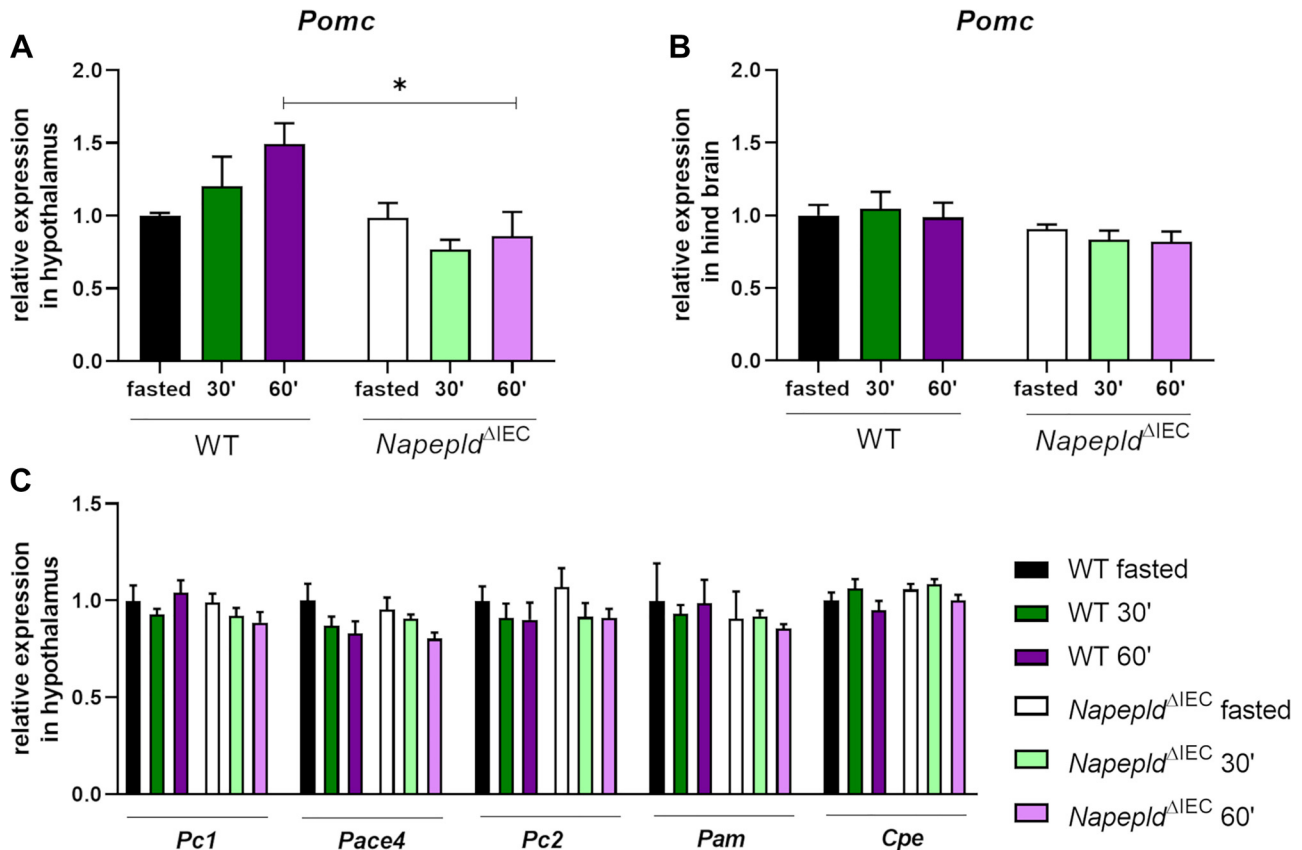


Fig. 2. Dysfunction of proopiomelanocortin (POMC) neurons occurs rapidly in the hypothalamus of *Napepld*^{ΔIEC} mice in response to lipid exposure. A: the mRNA expression of *Pomc* was progressively upregulated in the hypothalamus of wild-type (WT) mice following oral lipid load, whereas this response was defective in the hypothalamus of *Napepld*^{ΔIEC} mice, where *Pomc* mRNA remained unchanged over time ($n = 6-8$). B: the mRNA expression of *Pomc* in the hindbrain was unchanged comparing WT and *Napepld*^{ΔIEC} mice ($n = 5-8$). C: at transcriptional level, there was no difference in the expression of the enzymes involved in the post-translational cleavage of POMC ($n = 5-8$). Data are expressed as means \pm SE. * $P < 0.05$ according to 2-way ANOVA, followed by Tukey's post hoc test.

Napepld^{ΔIEC} mice in response to lipid challenge. After confirming the specificity of the deletion (Supplemental Fig. S3; <https://doi.org/10.6084/m9.figshare.12666344>), we examined several receptors mediating anorexigenic signals (Fig. 3A), such as receptors for gut hormones, namely cholecystokinin (*Cckar*), leptin (*Lepr*), GLP-1, and PYY (*Glp1r* and *Y2r*, respectively), and OEA receptor (*Gpr119*). We also investigated the neurotransmitter *Cart*, which is released by vagal afferences in the hindbrain to suppress appetite (Fig. 3A) (10, 28). We probed the orexigenic signals such as ghrelin receptor (*Ghsh*) and cannabinoid receptor 1 (*Cnr1*) (Fig. 3B). Overall, no major difference was observed at the transcriptional level for any of the receptors or neurotransmitters studied.

Additionally, in another experiment, we quantified c-fos-positive (c-fos⁺) neurons, markers of neuronal activation, 1 h after HFD exposure. We chose this time point based on previous study showing that c-fos expression in the brain peaks between 1 and 2 h after feeding (51). After an overnight fast, we exposed WT and *Napepld*^{ΔIEC} mice to HFD and quantified c-fos in the nucleus of the solitary tract (NTS), the relay station for vagal terminations in the hindbrain. There was no difference in the number of neurons activated in the NTS of WT and *Napepld*^{ΔIEC} mice in response to HFD (Fig. 3C).

Altogether, these results showed that the alteration of the anorexigenic regulatory signal in the hypothalamus is not due to a defect in vagal sensing or to an impaired vagal conveyance of information from the gut to the brain.

Napepld^{ΔIEC} Mice Have Submaximal Response to Endogenous GLP-1

In the last decade, several studies have been showing the existence of a close link between OEA and GLP-1. A first line of evidence suggested that OEA binds and activates GPR119 receptor on enteroendocrine L cells, thus stimulating the release of GLP-1 (26, 27). Additionally, it has recently been described that OEA itself regulates GLP-1 receptor (GLP-1R) signaling (3). Indeed, in vitro, OEA specifically binds to GLP-1(7–36) amide (i.e., active GLP-1), thus creating a complex that induces a more powerful activation of GLP-1R in comparison with the action of GLP-1 alone (3).

In our model, *Napepld* deletion in intestinal epithelial cells impairs OEA mobilization in response to oral lipid. In WT mice, jejunal OEA content increased 60% and 70% at 30 and 60 min, respectively, after oral lipid load, whereas *Napepld*^{ΔIEC} displayed a delayed kinetic of OEA mobilization (Supplemental Fig. S4; <https://doi.org/10.6084/m9.figshare.12666353>). Additionally, the

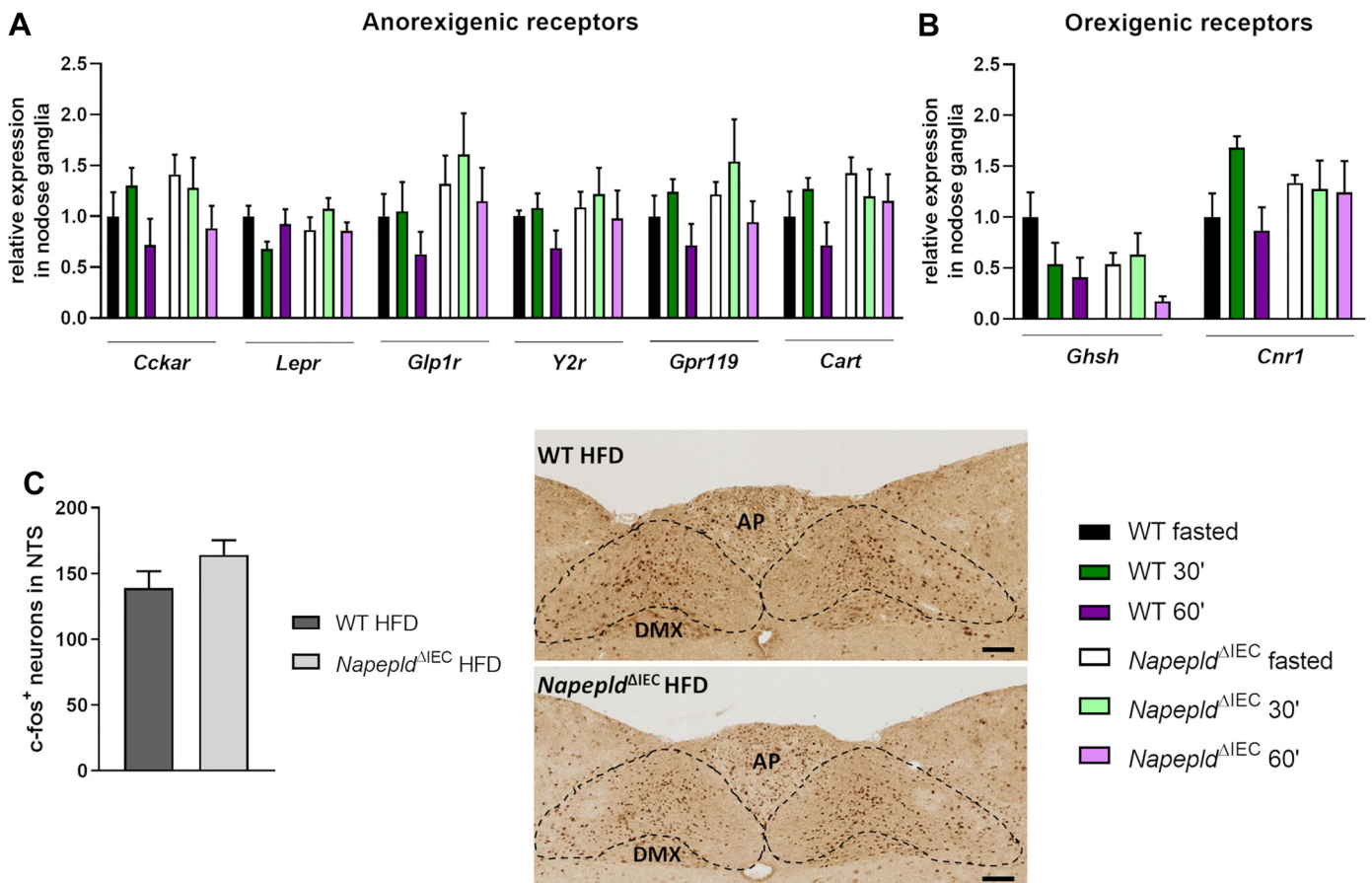


Fig. 3. Neither vagal plasticity nor vagal signaling is impaired by intestinal deletion of *Napepld* in response to lipid. Rapidly after the lipid challenge, the expression of receptors mediating appetite-suppressing (A) or appetite-stimulating (B) signals via the vagus nerve did not differ strikingly in comparing WT and *Napepld*^{ΔIEC} mice ($n = 5-8$). C, left: quantification of c-fos-positive (c-fos⁺) active neurons (dark brown staining) in the nucleus of the solitary tract (NTS) of wild-type (WT) and *Napepld*^{ΔIEC} mice following 1 h of HFD feeding ($n = 7-10$). C, right: representative bright-field images of the NTS, $\times 10$ magnification. Scale bar, 100 μ m. Black dashed lines circumscribe the NTS. AP, area postrema; DMX, dorsal motor nucleus of the vagus nerve. Data are expressed as means \pm SE. Statistical analysis: A and B, 2-way ANOVA; C, unpaired Student's *t*-test.

levels of peripheral circulating OEA increased in the WT mice 60 min after the lipid load, whereas the plasma levels of OEA in *Napepld*^{ΔIEC} mice remained similar to the fasted state even after lipid administration (Fig. 4A).

Therefore, considering that GLP-1 exerts appetite-suppressing action (1, 34) and that *Napepld*^{ΔIEC} mice have impaired lipid-induced OEA release (Fig. 4 and Supplemental Fig. S4) (14), we investigated whether the hyperphagia observed in *Napepld*^{ΔIEC} mice upon exposure to a lipid-rich diet could be the consequence of impaired GLP-1 secretion or signaling.

We explored the expression of *Gpr119* in the colon of WT and *Napepld*^{ΔIEC} mice and also the secretion of total GLP-1 in the portal vein in response to oral lipid stimulation. We found that *Gpr119* expression was unchanged in all conditions (Fig. 4B) and that total GLP-1 levels were similarly changed in WT and *Napepld*^{ΔIEC} mice in response to oral lipid (Fig. 4C).

Lack of GLP-1 appetite-suppressing action could also be the consequence of increased GLP-1 inactivation via dipeptidyl peptidase-4 (DPP-4). However, WT and *Napepld*^{ΔIEC} mice had similar DPP-4 activity in peripheral blood (Fig. 4D), concluding

that increased GLP-1 inactivation likely does not explain the hyperphagia observed in *Napepld*^{ΔIEC} mice.

It was recently demonstrated in vitro that OEA enhances GLP-1 potency in activating GLP-1R (3). Therefore, we hypothesized that *Napepld*^{ΔIEC} mice have less powerful activation of GLP-1R in comparison with WT given the lower level of OEA.

To explore this, we used exendin-4 (Ex-4), an agonist of GLP-1R whose potency is unaltered by OEA (2, 3). After an overnight fast, we injected WT and *Napepld*^{ΔIEC} mice with exendin-4 and precisely monitored HFD consumption over time by using metabolic cages. We chose to administer a dose of Ex-4 described to mildly suppress food intake (46) to mimic a physiological action as closely as possible.

Comparing the cumulative food intake at 2, 4, and 8 h postinjection, we observed that at each time point *Napepld*^{ΔIEC} mice injected with saline consumed between 30 and 43% more HFD than WT mice injected with saline (Fig. 5, A–C). Moreover, in WT mice, Ex-4 reduced food intake by 31 to 26% at 2 and 8 h, respectively, in comparison with the WT NaCl group (Fig. 5A–

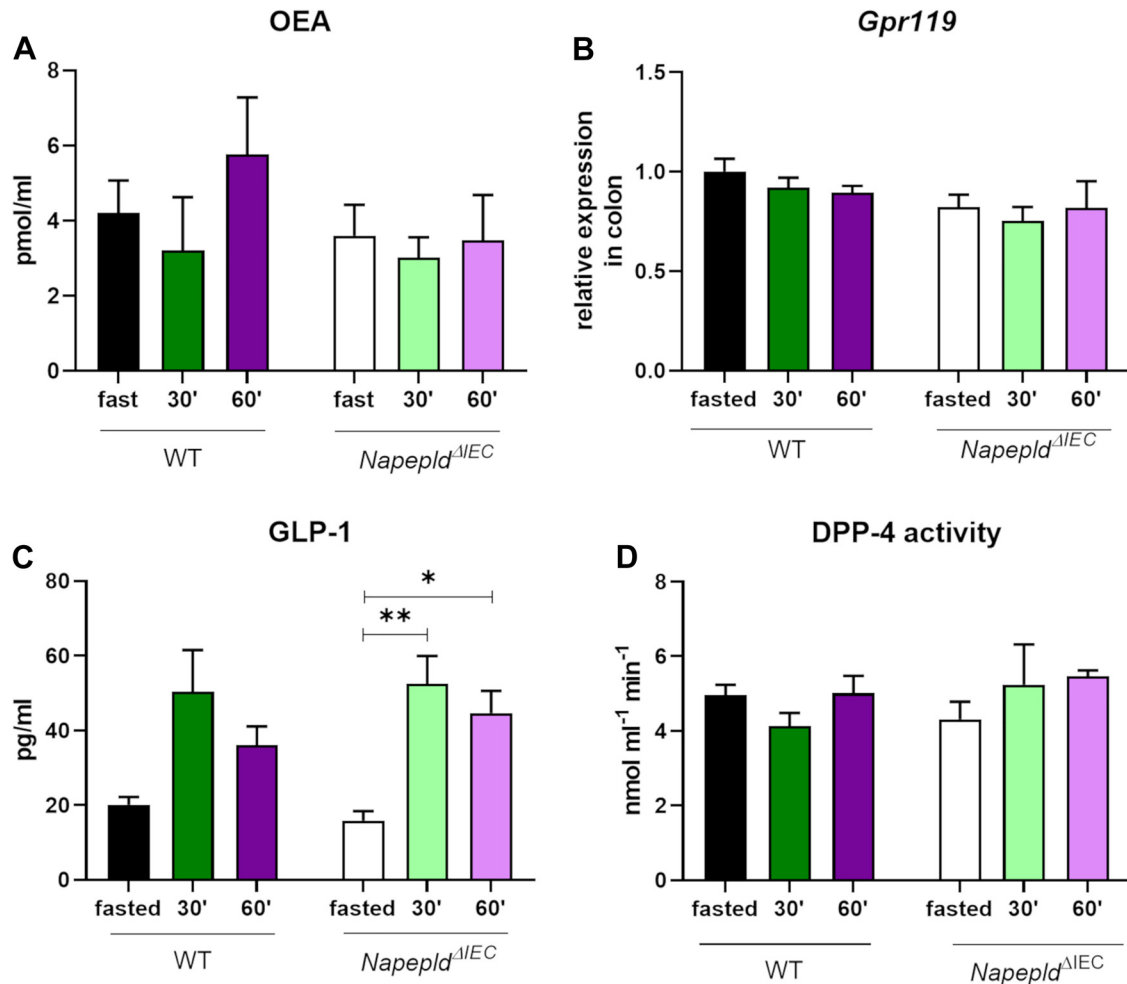


Fig. 4. *Napepld*^{ΔIEC} mice have impaired intestinal *N*-oleoylethanolamine (OEA) mobilization and do not display altered glucagon-like peptide-1 (GLP-1) secretion or inactivation. A: OEA (pmol/mL) measured in the plasma of the cava vein ($n = 4-8$). B: wild-type (WT) and *Napepld*^{ΔIEC} mice have similar expression of *Gpr119* in the colon ($n = 7$). C: quantification of total GLP-1 in the portal plasma of WT and *Napepld*^{ΔIEC} mice 30 and 60 min after lipid challenge. The level of GLP-1 similarly evolve in WT and *Napepld*^{ΔIEC} mice over time ($n = 6-8$). D: quantification of dipeptidyl peptidase-4 (DPP-4) activity in the peripheral blood of WT and *Napepld*^{ΔIEC} mice following nutritional stimulus. The activity of DPP-4 is not affected by the deletion or by the lipid challenge ($n = 6-8$). Data are expressed as means \pm SE. * $P < 0.05$ and ** $P < 0.01$ according to 2-way ANOVA, followed by Tukey's post hoc test.

C), confirming that the dose used has mild anorexigenic effect (46). Interestingly, this same dose of Ex-4 halves HFD consumption in *Napepld*^{ΔIEC} mice at 2 and 4 h (Fig. 5, A and B), with a tendency after 8 h ($P = 0.09$; Fig. 5C). Importantly, at each time point investigated, *Napepld*^{ΔIEC} Ex-4 mice consumed a similar amount of HFD as WT animals (Fig. 5, A–C), meaning that the administration of GLP-1R agonist that fully activates GLP-1R even in the absence of OEA prevented the hyperphagia developed by the intestinal deletion of NAPE-PLD.

Collectively, these results suggested that *Napepld*^{ΔIEC} mice displayed only partial activation of GLP-1R signaling via endogenous GLP-1, likely due to the diminished level of OEA.

DISCUSSION

We have previously observed that mice lacking *Napepld* in intestinal epithelial cells displayed hyperphagia within 4 h after the exposure to HFD. The hyperphagia occurred together with an impaired mRNA expression of POMC in the arcuate nucleus (ARC). These results suggested that intestinal NAPE-PLD contributes to control of lipid consumption. Although the existence of such a gut-to-brain axis has been proposed previously, the mechanisms behind it are still unknown.

In this study, we discovered a potential mechanism responsible for the aberrant gut to brain signaling characterizing the *Napepld*^{ΔIEC} mice. By exploring the hypothalamic response to lipids and examining the nervous and the endocrine component of the gut-to-brain axis following oral lipid exposure, we found that intestinal NAPE-PLD is a key sensor controlling not only the intestinal endocannabinoid system but also the integration of different peripheral satiety signals in the brain.

We observed that the level of two key NAEs regulating appetite, AEA and OEA (21), were differently regulated in the hypothalamus of WT and *Napepld*^{ΔIEC} in response to the HFD feeding after a fasting period. Upon HFD exposure, *Napepld*^{ΔIEC} mice had increased levels of AEA and reduced levels OEA as compared with WT mice. This finding likely contributes to explain the phenotype observed since AEA exerts an appetite-stimulating effect, whereas OEA decreases food intake (14). We noticed that the changes in the levels of NAEs in the brain were

restricted to NAEs regulating appetite and did not affect other members of the NAE family, such as PEA and SEA, which have been ascribed mainly to other effects and only mild appetite-suppressing action (21, 31, 41, 48). Furthermore, 2-AG, an orexiogenic bioactive lipid belonging to the endocannabinoid system but not to the cluster of NAEs, was not affected, suggesting that the alteration specifically involves the NAE cluster.

It is important to note that the deletion of *Napepld* is exclusively restricted to the intestinal epithelial cells and that the lower hypothalamic levels of OEA cannot be explained by a defect in local NAPE-PLD since its expression in the brain was similar between WT and *Napepld*^{ΔIEC} mice.

Furthermore, we observed that AEA and OEA impairment specifically occurred when *Napepld*^{ΔIEC} mice were exposed to a lipid-rich diet and not when they were refed with a normal diet. These results suggested that animals deleted for the intestinal *Napepld* have impaired regulation of hypothalamic appetite-regulating NAEs in response to their exposure to a lipid-rich diet and that NAPE-PLD acts specifically as an intestinal lipid sensor involved in the short-term regulation of food intake.

The expression of the main NAE-synthesizing and degrading enzymes was differently regulated in WT and *Napepld*^{ΔIEC} mice following HFD consumption. Alternative synthetic pathways for NAEs have also been described (33); however, the hypothalamic expression of enzymes involved in these pathways (namely *Abhd4*, *Gde1*) was not affected in our model (data not shown).

In our previous work, we found that intestinal deletion of *Napepld* was associated with a higher food intake, a lower expression of *Pomc* mRNA in the brain after 4 h of HFD exposure, and altered c-fos-positive neurons in the ARC and the paraventricular nucleus of the hypothalamus (PVN) (14). The major limitation of these preliminary observations is that measurements were performed only after 4 h of HFD consumption, a tardy time point that does not fully reflect the rapidity of physiological changes regulating food intake.

Therefore, in the present study, we dissected the mechanisms responsible for the hyperphagia. To do so, we chose to investigate hypothalamic response to intestinal lipid at early time points, namely 30 and 60 min after oral lipid challenge. Administration

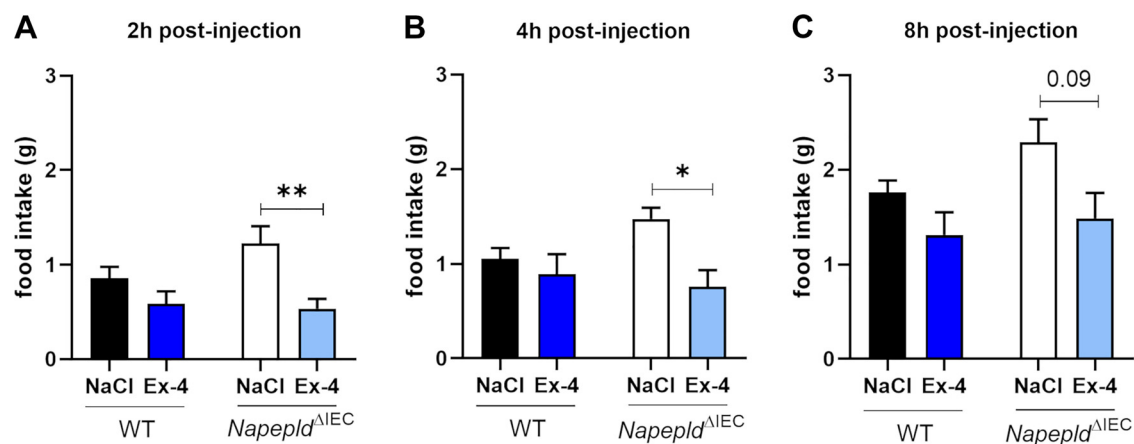


Fig. 5. *Napepld*^{ΔIEC} mice have submaximal responses to endogenous glucagon-like peptide-1 (GLP-1). A–C: cumulative consumption of high-fat diet (HFD) by wild-type (WT) and *Napepld*^{ΔIEC} mice upon administration of GLP-1 receptor agonist [exendin-4 (Ex-4)] or vehicle (NaCl). Two-, 4-, and 8-h postinjection Ex-4 halves HFD consumption of *Napepld*^{ΔIEC} mice, rescuing the hyperphagic phenotype ($n = 5–7$). Data are expressed as means \pm SE. * $P < 0.05$ and ** $P < 0.01$ according to 2-way ANOVA, followed by Tukey's post hoc test.

of lipid-rich emulsion by oral gavage allowed us to perfectly control the quantity of lipids given to each animal and let us exclude the contribution of both orosensing and mechano-sensing (from the stomach) inputs. This ensures that the observations made are depending primarily on intestinal sensing of lipids.

Using this method, we found that WT mice physiologically upregulated *Pomc* in the hypothalamus, whereas *Napepld*^{ΔIEC} did not. These results corroborate the data observed after 4 h of fat exposure and, more importantly, demonstrate that the impairment of *Pomc* mRNA expression is an early event occurring in the hypothalamus of *Napepld*^{ΔIEC} mice. We also confirmed that, among the appetite-regulating neuropeptides, the impaired response to lipid was exclusively restricted to POMC.

Few neurons expressing POMC are also present in the NTS located in the hindbrain. Despite their role not being fully elucidated yet, they are thought to contribute to the regulation of food intake (5, 40). When comparing WT and *Napepld*^{ΔIEC} mice, there was no difference in the evolution of *Pomc* mRNA expression in the NTS, demonstrating that the impairment of POMC transcription is likely hypothalamic specific.

Depending on energy requirements, POMC is cleaved into several distinct bioactive peptides, such as appetite-suppressing α -melanocyte stimulating hormone (α -MSH) (40). However, the expression of the enzymes involved in these posttranscriptional modifications did not differ in WT and *Napepld*^{ΔIEC} mice following lipid exposure.

The alteration of hypothalamic anorexigenic response in *Napepld*^{ΔIEC} mice occurred very rapidly; therefore, we hypothesized that impaired responsiveness of the vagus nerve to intestinal signals could contribute to the phenotype.

The vagus nerve is the only nerve connecting the intestine directly to the brain. A vast set of receptors expressed by vagal afferent neurons has recently been characterized (11). Together, receptors for gut peptides, bioactive lipids, and nutrients contribute to vagal sensing mechanisms. The array of receptors expressed by vagal afferent neurons can be modified in response to diet, a process known as vagal plasticity (8, 10). Up to now, this process has been described mainly in rats, and to our knowledge, only few studies have characterized vagal plasticity in mice (38, 52).

In our study, no difference was observed in transcriptional regulation of a representative set of receptors between WT and *Napepld*^{ΔIEC} mice. We could thus conclude that the vagal plasticity in response to lipid is not impaired by the intestinal deletion of *Napepld*. However, we may not exclude that for some of the receptors investigated, vagal plasticity is not only under transcriptional regulation but also under the control of membrane-to-vesicles trafficking (42).

Given this potential limitation, we used a complementary approach to investigate whether the conveyance of satiety signal from the intestine to the brain was altered by the deletion of intestinal *Napepld*. We quantified the number of c-fos-positive neurons in the NTS of WT and *Napepld*^{ΔIEC} mice after 1 h of HFD feeding, but no difference in the number of activated neurons was observed.

Overall, these results suggest that the intestinal deletion of *Napepld* does not impair either vagal sensitivity to intestinal content or vagal signaling from the intestine to the brain.

Gut hormones contribute to the fine-tuning of food intake via paracrine action by activating the receptors located on vagal terminations but also via endocrine activity, reaching the brain

through the bloodstream (19, 35). Among them, GLP-1 is recognized for its appetite-suppressing action (1, 34). GLP-1 secretion and binding of GLP-1 to its receptor are modulated by OEA. In detail, OEA activates GPR119 receptor expressed on the L cells and triggers GLP-1 release (4, 27, 32). In addition, recent evidence suggests that GLP-1(7–36) amide (i.e., active GLP-1) interacts with OEA, creating a complex with increased potency to activate GLP-1R (2, 3). Importantly, among the different NAEs tested, OEA is the only one having this activity (3). Notably, the role of AEA in this contest has not been investigated yet.

Because we found that *Napepld*^{ΔIEC} mice showed a delayed intestinal release of OEA when challenged with lipid, we speculated that the OEA-mediated GLP-1 release upon nutritional stimulation could be impaired in *Napepld*^{ΔIEC} mice. In our study, portal GLP-1 levels were similar between WT and *Napepld*^{ΔIEC} mice in response to lipid challenge. The similar profile of GLP-1 secretion, despite impaired intestinal OEA mobilization, was not the consequence of a compensatory upregulation of *Gpr119* in the colon of *Napepld*^{ΔIEC} mice. These results strongly suggest that in vivo endogenous intestinal OEA only partially contributes to GLP-1 release and thereby contrasts with the results found in vitro by Moss et al. (32) in GPR119-deficient L cells.

Despite exhibiting a normal level of portal GLP-1, *Napepld*^{ΔIEC} mice displayed a hyperphagic phenotype in comparison with WT mice. Therefore, we wondered whether increased GLP-1 inactivation via augmented DPP-4 activity could explain the lack of appetite-suppressing action in *Napepld*^{ΔIEC} mice. However, DPP-4 activity was unchanged when comparing WT and *Napepld*^{ΔIEC} mice. Therefore, this set of data suggested that the hyperphagic phenotype displayed by *Napepld*^{ΔIEC} mice was the consequence of neither impaired GLP-1 release nor higher GLP-1 inactivation. Hence, we questioned the potential activity of GLP-1 in *Napepld*^{ΔIEC} mice.

Considering that recent data have shown that GLP-1 and OEA form a complex to activate GLP-1R (3), we hypothesized that the defective intestinal lipid-induced mobilization of OEA and the diminished circulating level of OEA observed in *Napepld*^{ΔIEC} mice could impair the formation of this GLP-1:OEA complex and eventually lead to submaximal activation of GLP-1R and partial inhibition of appetite. To explore this hypothesis, we used Ex-4, a GLP-1R agonist. Importantly, Ex-4 alone maximally activates GLP-1R (2), and the potency of Ex-4 is unaltered by the addition of OEA (3). Ex-4 administration prevented the hyperphagia of *Napepld*^{ΔIEC} mice upon their exposure to HFD, and they consumed the same amount of HFD as WT mice. This implicates that a maximal activation of GLP-1R is sufficient to prevent the impairment of NAPE-PLD-mediated control of food intake via the gut-to-brain axis. In other words, we postulate that the decreased intestinal and circulating OEA levels due to the deletion of *Napepld* in the intestinal epithelial cells cause a submaximal activation of GLP-1R, leading to a partial appetite-suppressing action of GLP-1.

Increasing amounts of evidence suggest that GLP-1 acts on POMC neurons in the ARC. Secher et al. (44) showed that active GLP-1 modulated the firing of hypothalamic neurons by directly activating POMC/CART neurons and inhibiting NPY/AgRP neurons via a GABA-dependent action. These observations were also recently confirmed by others (23). Moreover, GLP-1R agonists administered peripherally or centrally also influence the firing or the transcriptional activity of neurons in

the ARC (7, 37, 44). Those responses relied on GLP-1R, since the effects were lost in GLP-1-deficient mice or by the administration of GLP-1 receptor inhibitor (7, 44).

Combining these observations with our own data, we speculate that the defective upregulation of *Pomc* in the hypothalamus of *Napepld*^{ΔIEC} mice is the consequence of a submaximal activation of GLP-1R in the ARC that could be due to the decreased amount of GLP-1:OEA complex in our animal model.

This assumption is supported by other observations. First, once captured in the GLP-1:OEA complex, GLP-1 undergoes a conformational change that alters its susceptibility to cleavage (3). Consequently, it is probable that the GLP-1:OEA complex has a prolonged half-life compared with GLP-1 or OEA alone. Second, peripherally administered GLP-1R agonists have been shown to reach all circumventricular organs (CVO) and enter the PVN and ARC as well (44). Similarly, the GLP-1:OEA complex could reach the ARC and directly influence neuronal populations therein.

Within the NTS, GLP-1-expressing neurons are considered important regulators of energy intake. These neurons are activated by peripheral signals and project to other brain centers that express GLP-1R and are important in food intake regulation, including ARC (49). Given the reduced level of OEA in the hypothalamus of *Napepld*^{ΔIEC} mice following HFD feeding, we may not rule out that the formation of the GLP-1:OEA complex could also be blunted centrally and eventually further contribute to a lower activation of GLP-1R in the ARC.

In conclusion, by using our mouse model of inducible intestinal deletion of *Napepld*, we unraveled novel physiological mechanisms of the gut-to-brain axis regulating food intake. We highlighted the importance of intestinal epithelial cell NAPE-PLD in the early mechanisms regulating food intake upon lipid exposure. We also pointed out the involvement of intestinal NAPE-PLD in the regulation of hypothalamic OEA and AEA. Despite a normal GLP-1 secretion, the altered intestinal, circulating, and hypothalamic OEA mobilization likely contributes to reduce the GLP-1R activation, thereby suggesting that the hypophagic action of OEA is not only ascribed to the lipid per se but also relies on the interaction of OEA with the intestinal peptide GLP-1. This set of experiments highlights the complex mechanism of action involved in the fine-tuning of appetite and further reinforces the knowledge regarding the impact of dietary lipids on the food intake behavior.

ACKNOWLEDGMENTS

We thank A. Puel, H. Danthinne, A. Barrois, and M. Goebbels for excellent technical assistance. We thank A. Paquot from the Bioanalysis and Pharmacology of Bioactive Lipids Research Group (BPBL) at the Louvain Drug Research Institute (LDRI; UCLouvain, Brussels, Belgium) for help. We thank C. Bouzin and A. Daumerie from the imagery platform 2IP from the Institut de Recherche Expérimentale et Clinique (IREC; UCLouvain, Brussels, Belgium) for their excellent help and N. Van Baren for the use of the Panoramic imagery system at the De Duve institute (DDUV; UCLouvain, Brussels, Belgium).

M. Rastelli is a research fellow at FRS-FNRS (Fonds de la Recherche Scientifique), Belgium. P. D. Cani is a senior research associate at FRS-FNRS, Belgium.

GRANTS

This work was supported by the Fonds de la Recherche Scientifique (FNRS FRFS-WELBIO) under Grants WELBIO-CR-2017C-02 and WELBIO-CR-2019C-02R and the Funds Baillet-Latour under the Grant For Medical Research 2015.

DISCLOSURES

No conflicts of interest, financial or otherwise, are declared by the authors.

AUTHOR CONTRIBUTIONS

M. Rastelli and P.D.C. conceived and designed research; M. Rastelli, M.V.H., R.T., C.L., M. Régnier, D.B., and G.G.M., performed experiments; M. Rastelli, G.G.M., and P.D.C. analyzed data; M. Rastelli, R.N., and P.D.C., interpreted results of experiments; M. Rastelli prepared figures; M. Rastelli and P.D.C. drafted manuscript; M. Rastelli, M.V.H., R.T., C.L., M. Régnier, D.B., N.M.D., A.E., R.N., S.L., G.G.M., and P.D.C. edited and revised manuscript; M. Rastelli, M.V.H., R.T., C.L., M. Régnier, D.B., N.M.D., A.E., R.N., S.L., G.G.M., and P.D.C. approved final version of manuscript.

REFERENCES

1. Baggio LL, Drucker DJ. Glucagon-like peptide-1 receptors in the brain: controlling food intake and body weight. *J Clin Invest* 124: 4223–4226, 2014. doi:10.1172/JCI78371.
2. Brown JD, McAnally D, Ayala JE, Burmeister MA, Morfa C, Smith L, Ayala JE. Oleylethanolamide modulates glucagon-like peptide-1 receptor agonist signaling and enhances exendin-4-mediated weight loss in obese mice. *Am J Physiol Regul Integr Comp Physiol* 315: R595–R608, 2018. doi:10.1152/ajpregu.00459.2017.
3. Cheng YH, Ho MS, Huang WT, Chou YT, King K. Modulation of glucagon-like peptide-1 (GLP-1) potency by endocannabinoid-like lipids represents a novel mode of regulating GLP-1 receptor signaling. *J Biol Chem* 290: 14302–14313, 2015. doi:10.1074/jbc.M115.655662.
4. Chu ZL, Carroll C, Alfonso J, Gutierrez V, He H, Lucman A, Pedraza M, Mondala H, Gao H, Bagnol D, Chen R, Jones RM, Behan DP, Leonard J. A role for intestinal endocrine cell-expressed G protein-coupled receptor 119 in glycemic control by enhancing glucagon-like peptide-1 and glucose-dependent insulinotropic peptide release. *Endocrinology* 149: 2038–2047, 2008. doi:10.1210/en.2007-0966.
5. Cone RD. Anatomy and regulation of the central melanocortin system. *Nat Neurosci* 8: 571–578, 2005. doi:10.1038/nn1455.
6. Cristino L, Becker T, Di Marzo V. Endocannabinoids and energy homeostasis: an update. *Biofactors* 40: 389–397, 2014. doi:10.1002/biof.1168.
7. Dalvi PS, Nazarians-Armavil A, Purser MJ, Belsham DD. Glucagon-like peptide-1 receptor agonist, exendin-4, regulates feeding-associated neuropeptides in hypothalamic neurons in vivo and in vitro. *Endocrinology* 153: 2208–2222, 2012. doi:10.1210/en.2011-1795.
8. de Lartigue G. Role of the vagus nerve in the development and treatment of diet-induced obesity. *J Physiol* 594: 5791–5815, 2016. doi:10.1113/JP271538.
9. DiPatrizio NV. Endocannabinoids in the gut. *Cannabis Cannabinoid Res* 1: 67–77, 2016. doi:10.1089/can.2016.0001.
10. Dockray GJ. The versatility of the vagus. *Physiol Behav* 97: 531–536, 2009. doi:10.1016/j.physbeh.2009.01.009.
11. Egerod KL, Petersen N, Timshel PN, Rekling JC, Wang Y, Liu Q, Schwartz TW, Gautron L. Profiling of G protein-coupled receptors in vagal afferents reveals novel gut-to-brain sensing mechanisms. *Mol Metab* 12: 62–75, 2018. doi:10.1016/j.molmet.2018.03.016.
12. El Marjou F, Janssen KP, Chang BH, Li M, Hindie V, Chan L, Louvard D, Chambon P, Metzger D, Robine S. Tissue-specific and inducible Cre-mediated recombination in the gut epithelium. *Genesis* 39: 186–193, 2004. doi:10.1002/gene.20042.
13. Esposito G, Capoccia E, Turco F, Palumbo I, Lu J, Steardo A, Cuomo R, Sarnelli G, Steardo L. Palmitoylethanolamide improves colon inflammation through an enteric glia/Toll like receptor 4-dependent PPAR-α activation. *Gut* 63: 1300–1312, 2014. doi:10.1136/gutjnl-2013-305005.
14. Everard A, Plovier H, Rastelli M, Van Hul M, de Wouters d'Oplinter A, Geurts L, Druart C, Robine S, Delzenne NM, Muccioli GG, de Vos WM, Luquet S, Flamand N, Di Marzo V, Cani PD. Intestinal epithelial N-acylphosphatidylethanolamine phospholipase D links dietary fat to metabolic adaptations in obesity and steatosis. *Nat Commun* 10: 457, 2019. doi:10.1038/s41467-018-08051-7.
15. Fu J, Gaetani S, Oveisi F, Lo Verme J, Serrano A, Rodríguez De Fonseca F, Rosengarth A, Luecke H, Di Giacomo B, Tarzia G, Piomelli D. Oleylethanolamide regulates feeding and body weight through activation of the nuclear receptor PPAR-α. *Nature* 425: 90–93, 2003. doi:10.1038/nature01921.

16. Fu J, Kim J, Oveisi F, Astarita G, Piomelli D. Targeted enhancement of oleoylethanolamide production in proximal small intestine induces across-meal satiety in rats. *Am J Physiol Regul Integr Comp Physiol* 295: R45–R50, 2008. doi:10.1152/ajpregu.00126.2008.
17. Gaetani S, Oveisi F, Piomelli D. Modulation of meal pattern in the rat by the anorexic lipid mediator oleoylethanolamide. *Neuropsychopharmacology* 28: 1311–1316, 2003. doi:10.1038/sj.npp.1300166.
18. Geurts L, Everard A, Van Hul M, Essaghir A, Duparc T, Matamoros S, Plovier H, Castel J, Denis RG, Bergiers M, Druart C, Alhouayek M, Delzenne NM, Muccioli GG, Demoulin JB, Luquet S, Cani PD. Adipose tissue NAPE-PLD controls fat mass development by altering the browning process and gut microbiota. *Nat Commun* 6: 6495, 2015. doi:10.1038/ncomms7495.
19. Gribble FM, Reimann F. Enteroendocrine cells: chemosensors in the intestinal epithelium. *Annu Rev Physiol* 78: 277–299, 2016. doi:10.1146/annurev-physiol-021115-105439.
20. Hansen HS. Role of anorectic N-acylethanolamines in intestinal physiology and satiety control with respect to dietary fat. *Pharmacol Res* 86: 18–25, 2014. doi:10.1016/j.phrs.2014.03.006.
21. Hansen HS, Diep TA. N-acylethanolamines, anandamide and food intake. *Biochem Pharmacol* 78: 553–560, 2009. doi:10.1016/j.bcp.2009.04.024.
22. Hansen HS, Vana V. Non-endocannabinoid N-acylethanolamines and 2-monoacylglycerols in the intestine. *Br J Pharmacol* 176: 1443–1454, 2019. doi:10.1111/bph.14175.
23. He Z, Gao Y, Lieu L, Afrin S, Cao J, Michael NJ, Dong Y, Sun J, Guo H, Williams KW. Direct and indirect effects of liraglutide on hypothalamic POMC and NPY/AgRP neurons - Implications for energy balance and glucose control. *Mol Metab* 28: 120–134, 2019. doi:10.1016/j.molmet.2019.07.008.
24. Inoue M, Tsuboi K, Okamoto Y, Hidaka M, Uyama T, Tsutsumi T, Tanaka T, Ueda N, Tokumura A. Peripheral tissue levels and molecular species compositions of N-acyl-phosphatidylethanolamine and its metabolites in mice lacking N-acyl-phosphatidylethanolamine-specific phospholipase D. *J Biochem* 162: 449–458, 2017. doi:10.1093/jb/mvx054.
25. Izzo AA, Sharkey KA. Cannabinoids and the gut: new developments and emerging concepts. *Pharmacol Ther* 126: 21–38, 2010. doi:10.1016/j.pharmthera.2009.12.005.
26. Lan H, Vassileva G, Corona A, Liu L, Baker H, Golovko A, Abbondanzo SJ, Hu W, Yang S, Ning Y, Del Vecchio RA, Poulet F, Laverty M, Gustafson EL, Hedrick JA, Kowalski TJ. GPR119 is required for physiological regulation of glucagon-like peptide-1 secretion but not for metabolic homeostasis. *J Endocrinol* 201: 219–230, 2009. doi:10.1677/JOE-08-0453.
27. Lauffer LM, Iakoubov R, Brubaker PL. GPR119 is essential for oleoylethanolamide-induced glucagon-like peptide-1 secretion from the intestinal enteroendocrine L-cell. *Diabetes* 58: 1058–1066, 2009. doi:10.2337/db08-1237.
28. Lee SJ, Krieger JP, Vergara M, Quinn D, McDougale M, de Araujo A, Darling R, Zollinger B, Anderson S, Pan A, Simonnet EJ, Pignalosa A, Arnold M, Singh A, Langhans W, Raybould HE, de Lartigue G. Blunted vagal cocaine- and amphetamine-regulated transcript promotes hyperphagia and weight gain. *Cell Reports* 30: 2028–2039.e4, 2020. doi:10.1016/j.celrep.2020.01.045.
29. Leung D, Saghatelian A, Simon GM, Cravatt BF. Inactivation of N-acyl phosphatidylethanolamine phospholipase D reveals multiple mechanisms for the biosynthesis of endocannabinoids. *Biochemistry* 45: 4720–4726, 2006. doi:10.1021/bi0601631.
30. Maccarrone M, Bab I, Bíró T, Cabral GA, Dey SK, Di Marzo V, Konje JC, Kunos G, Mechoulam R, Pacher P, Sharkey KA, Zimmer A. Endocannabinoid signaling at the periphery: 50 years after THC. *Trends Pharmacol Sci* 36: 277–296, 2015. doi:10.1016/j.tips.2015.02.008.
31. Maccarrone M, Carboni A, Parolaro D, Margonelli A, Massi P, Bari M, Battista N, Finazzi-Agrò A. Cannabimimetic activity, binding, and degradation of stearoylethanolamide within the mouse central nervous system. *Mol Cell Neurosci* 21: 126–140, 2002. doi:10.1006/mcne.2002.1164.
32. Moss CE, Glass LL, Diakogiannaki E, Pais R, Lenaghan C, Smith DM, Wedin M, Bohlooly-Y M, Gribble FM, Reimann F. Lipid derivatives activate GPR119 and trigger GLP-1 secretion in primary murine L-cells. *Peptides* 77: 16–20, 2016. doi:10.1016/j.peptides.2015.06.012.
33. Muccioli GG. Endocannabinoid biosynthesis and inactivation, from simple to complex. *Drug Discov Today* 15: 474–483, 2010. doi:10.1016/j.drudis.2010.03.007.
34. Müller TD, Finan B, Bloom SR, D'Alessio D, Drucker DJ, Flatt PR, Fritsche A, Gribble F, Grill HJ, Habener JF, Holst JJ, Langhans W, Meier JJ, Nauck MA, Perez-Tilve D, Pocai A, Reimann F, Sandoval DA, Schwartz TW, Seeley RJ, Stemmer K, Tang-Christensen M, Woods SC, DiMarchi RD, Tschöp MH. Glucagon-like peptide 1 (GLP-1). *Mol Metab* 30: 72–130, 2019. doi:10.1016/j.molmet.2019.09.010.
35. Murphy KG, Bloom SR. Gut hormones and the regulation of energy homeostasis. *Nature* 444: 854–859, 2006. doi:10.1038/nature05484.
36. Mutemberezi V, Masquelier J, Guillemot-Legris O, Muccioli GG. Development and validation of an HPLC-MS method for the simultaneous quantification of key oxysterols, endocannabinoids, and ceramides: variations in metabolic syndrome. *Anal Bioanal Chem* 408: 733–745, 2016. doi:10.1007/s00216-015-9150-z.
37. NamKoong C, Kim MS, Jang BT, Lee YH, Cho YM, Choi HJ. Central administration of GLP-1 and GIP decreases feeding in mice. *Biochem Biophys Res Commun* 490: 247–252, 2017. doi:10.1016/j.bbrc.2017.06.031.
38. Nefti W, Chaumontet C, Fromentin G, Tomé D, Darcel N. A high-fat diet attenuates the central response to within-meal satiation signals and modifies the receptor expression of vagal afferents in mice. *Am J Physiol Regul Integr Comp Physiol* 296: R1681–R1686, 2009. doi:10.1152/ajpregu.90733.2008.
39. Piomelli D. A fatty gut feeling. *Trends Endocrinol Metab* 24: 332–341, 2013. doi:10.1016/j.tem.2013.03.001.
40. Pritchard LE, Turnbull AV, White A. Pro-opiomelanocortin processing in the hypothalamus: impact on melanocortin signalling and obesity. *J Endocrinol* 172: 411–421, 2002. doi:10.1677/joe.0.1720411.
41. Rodríguez de Fonseca F, Navarro M, Gómez R, Escuredo L, Nava F, Fu J, Murillo-Rodríguez E, Giuffrida A, LoVerme J, Gaetani S, Kathuria S, Gall C, Piomelli D. An anorexic lipid mediator regulated by feeding. *Nature* 414: 209–212, 2001. doi:10.1038/35102582.
42. Ronveaux CC, de Lartigue G, Raybould HE. Ability of GLP-1 to decrease food intake is dependent on nutritional status. *Physiol Behav* 135: 222–229, 2014. doi:10.1016/j.physbeh.2014.06.015.
43. Schneeberger M, Gomis R, Claret M. Hypothalamic and brainstem neuronal circuits controlling homeostatic energy balance. *J Endocrinol* 220: T25–T46, 2014. doi:10.1530/JOE-13-0398.
44. Secher A, Jelsing J, Baquero AF, Hecksher-Sørensen J, Cowley MA, Dalbøge LS, Hansen G, Grove KL, Pyke C, Raun K, Schäffer L, Tang-Christensen M, Verma S, Witgen BM, Vrang N, Bjerre Knudsen L. The arcuate nucleus mediates GLP-1 receptor agonist liraglutide-dependent weight loss. *J Clin Invest* 124: 4473–4488, 2014. doi:10.1172/JCI75276.
45. Simon V, Cota D. Mechanisms in endocrinology: Endocannabinoids and metabolism: past, present and future. *Eur J Endocrinol* 176: R309–R324, 2017. doi:10.1530/EJE-16-1044.
46. Talsania T, Anini Y, Siu S, Drucker DJ, Brubaker PL. Peripheral extendin-4 and peptide YY(3-36) synergistically reduce food intake through different mechanisms in mice. *Endocrinology* 146: 3748–3756, 2005. doi:10.1210/en.2005-0473.
47. Tellez LA, Medina S, Han W, Ferreira JG, Licona-Limón P, Ren X, Lam TT, Schwartz GJ, de Araujo IE. A gut lipid messenger links excess dietary fat to dopamine deficiency. *Science* 341: 800–802, 2013. doi:10.1126/science.1239275.
48. Terrazzino S, Berto F, Dalle Carbonare M, Fabris M, Guiotto A, Bernardini D, Leon A. Stearoylethanolamide exerts anorexic effects in mice via down-regulation of liver stearoyl-coenzyme A desaturase-1 mRNA expression. *FASEB J* 18: 1580–1582, 2004. doi:10.1096/fj.03-1080fje.
49. Trapp S, Cork SC. PPG neurons of the lower brain stem and their role in brain GLP-1 receptor activation. *Am J Physiol Regul Integr Comp Physiol* 309: R795–R804, 2015. doi:10.1152/ajpregu.00333.2015.
50. Ueda N, Tsuboi K, Uyama T. Metabolism of endocannabinoids and related N-acylethanolamines: canonical and alternative pathways. *FEBS J* 280: 1874–1894, 2013. doi:10.1111/febs.12152.
51. Wu Q, Lemus MB, Stark R, Bayliss JA, Reichenbach A, Lockie SH, Andrews ZB. The temporal pattern of cfos activation in hypothalamic, cortical, and brainstem nuclei in response to fasting and refeeding in male mice. *Endocrinology* 155: 840–853, 2014. doi:10.1210/en.2013-1831.
52. Yuan X, Huang Y, Shah S, Wu H, Gautron L. Levels of cocaine- and amphetamine-regulated transcript in vagal afferents in the mouse are unaltered in response to metabolic challenges. *eNeuro* 3: ENEURO.0174-16.2016, 2016. doi:10.1523/ENEURO.0174-16.2016.